

NACA RM L54B22



RESEARCH MEMORANDUM

MEASUREMENTS OF NORMAL-FORCE-COEFFICIENT FLUCTUATION ON
FOUR 9-PERCENT-THICK AIRFOILS HAVING DIFFERENT
LOCATIONS OF MAXIMUM THICKNESS

By Milton D. Humphreys

Langley Aeronautical Laboratory
Langley Field, Va.

CLASSIFICATION CANCELLED

Authority 440 Res. 6b Date 2/8/56

KN 97

By Sm 264 3/16/56 See _____

CLASSIFIED DOCUMENT

This material contains information affecting the National Defense of the United States within the meaning of the espionage laws, Title 18, U.S.C., Secs. 793 and 794, the transmission or revelation of which in any manner to an unauthorized person is prohibited by law.

NATIONAL ADVISORY COMMITTEE
FOR AERONAUTICS

APR 28 1954

WASHINGTON

April 27, 1954

LANGLEY AERONAUTICAL LABORATORY
LIBRARY, NACA
LANGLEY FIELD, VIRGINIA

CONFIDENTIAL

NATIONAL ADVISORY COMMITTEE FOR AERONAUTICS

RESEARCH MEMORANDUM

MEASUREMENTS OF NORMAL-FORCE-COEFFICIENT FLUCTUATION ON
FOUR 9-PERCENT-THICK AIRFOILS HAVING DIFFERENT
LOCATIONS OF MAXIMUM THICKNESS

By Milton D. Humphreys

SUMMARY

A two-dimensional wind-tunnel investigation of the effects of maximum-thickness location on fluctuating pressures and normal-force coefficients on 9-percent-thick airfoils indicated that for normal-force coefficients up to 0.6 the section variables had little effect on the pressure pulsations and root-mean-square normal-force-coefficient fluctuations. At normal-force coefficients above 0.6, up to approximately the maximum normal-force coefficient, considerable reductions in root-mean-square normal-force fluctuations were obtained by using an airfoil having the maximum thickness located at or behind the 42.5-percent-chord station. From the standpoint of local panel loads, none of the airfoils had consistently lower fluctuating loads throughout the speed and normal-force-coefficient ranges. It appeared, however, that the NACA 65A009 airfoil would probably be the best choice of the sections tested for operation throughout the high subsonic Mach number range.

INTRODUCTION

Former investigations (for example, refs. 1 and 2) have provided useful information on the character and magnitude of the local pressure pulsations on airfoils at high subsonic speeds. These results can be used for the prediction of local panel loads, but the fluctuating normal-force coefficient of the section, which is of more significance in buffeting studies, cannot be obtained from the pressure-pulsation records unless detailed consideration is given to the phase relationships of the pressures at different chordwise stations. In the present study use is made of an electrical integrating device to obtain, from the pulsating-pressure measurements, the desired root-mean-square values of the fluctuating normal-force coefficient for several 9-percent-thick airfoils.

Previous pressure-pulsation studies for 6-percent-thick sections (ref. 1) indicated considerably lower pulsations for the NACA 65A006 section than for the NACA 64A006 section. In the present investigation, therefore, a range of maximum-thickness positions was covered by investigation of the NACA 63A009, 64A009, 65A009, and 16-009 sections. The tests covered a Mach number range of 0.5 to 1.0, angles of attack of 0° to 12° , and a Reynolds number range of 1.5×10^6 to 2.1×10^6 . The results of a somewhat similar investigation of different profiles are reported in reference 3.

SYMBOLS

M	free-stream Mach number
q	free-stream dynamic pressure, lb/sq ft
Δp	double-amplitude pressure pulsation, lb/sq ft
c_n	section normal-force coefficient
c_d	section drag coefficient
$\overline{\Delta p/q}$	chordwise average of $\Delta p/q$
$\overline{\Delta c_n}$	square root of mean square normal-force-coefficient fluctuations (unsteady component of the normal-force coefficient)
α	angle of attack, deg

APPARATUS, MODELS, AND TESTS

The investigation was conducted in the Langley 4- by 19-inch semiopen tunnel (fig. 1). Dried air at 20 pounds per square inch absolute flowed from the settling chamber through the test chamber and was discharged to the atmosphere through the diffuser. The test-section Mach number was regulated by a variable-area throat located in the diffuser downstream from the test section. The tunnel calibration and operation were similar to that described in reference 4.

Jet-boundary corrections for this type of test have not yet been determined at high subsonic Mach numbers; therefore no correction has been applied to any of these data. For incompressible potential flow the correction to the angle of attack is the major correction and is given (for the tunnel configuration used) by $\alpha_{\text{true}} = \alpha_{\text{test}} - 1.85c_n$.

Jet-boundary effects are discussed in more detail in references 4 and 5, where it is indicated that, except for the angle-of-attack correction, the jet-boundary effects are probably not large.

The 4-inch-chord models investigated and their position of maximum thickness are as follows:

Airfoil	Position of maximum thickness, percent chord
NACA 63A009	36.25
NACA 64A009	39.0
NACA 65A009	42.50
NACA 16-009	50.0

The model ordinates are given in reference 4. Pressure orifices were located on the upper surface of the models at the 3.1-, 14-, 25-, 37.5-, 50-, 62.5-, 75-, and 87.5-percent-chord stations. The lower-surface flow conditions were not investigated, since an earlier investigation (ref. 2) showed that under lifting conditions the major flow unsteadiness was on the upper surface of the airfoil. This may lead to inaccuracies in the force fluctuations at angles of attack near zero lift; however, in this region the fluctuations are small and inaccuracies of little significance.

Miniature electrical pressure gages and a recording system having a flat frequency response from 40 to 500 cycles per second were used to measure the fluctuating pressures at each of the eight pressure orifices along the chord of the airfoils. In the first phase of the investigation the electrical output of these gages was recorded to give the time history of the fluctuating pressures (as in fig. 2). From these records a typical or predominant double-amplitude value of the fluctuating pressure Δp was chosen by inspection (as in ref. 1) and plotted to give the distribution of $\Delta p/q$ along the airfoil chord (fig. 3). The data thus obtained are useful in the determination of predominant fluctuations of local panel loads.

In the second phase of the investigation the electrical outputs of the same miniature electrical pressure gages were added simultaneously by means of an electrical integrator, a dynamic version of the static integrator described in reference 6, to produce an electrical signal corresponding to the instantaneous fluctuating component of the normal force. These signals, over a period of time, were converted by a vacuum thermocouple and milliammeter into a meter reading corresponding to the square of the mean fluctuating normal force. This information was easily transposed into the root mean square of the fluctuating normal force (fig. 4). A laboratory calibration of the system indicated that the response was approximately 1 to 1 up to 300 cycles per second and was amplified considerably (up to 1.8 times at atmospheric pressure) between 300

and 1,000 cycles per second. The amplification was reduced considerably as the applied static pressure was reduced with increasing Mach number; hence, the component of the data contributed by the higher frequencies became more accurate at the higher Mach numbers. No correction for frequency response has been made to these data, since laboratory investigations have shown that only negligible phase lag existed in the measuring apparatus. Further, since all the eight gages, all orifices, and all tubing were practically identical, their phase characteristics would be identical and would have no effect on the integrated results.

To check the reproducibility of the root-mean-square normal-force fluctuation for a given test condition, three separate runs were made — two using the electrical integrator, and a third run from which the pressure record of figure 2 was mechanically integrated. The results of the mechanical integration yielded a root-mean-square normal-force-coefficient fluctuation of 0.055, which compares favorably with electrically integrated values from two other tests of 0.043 and 0.060 for this test point (fig. 5). The repeatability for three separate tests obtained at a Reynolds number of 1.9×10^6 and at maximum normal-force coefficient is excellent, in view of the very unsteady nature of the flow phenomenon measured at this test condition.

Pressure-pulsation data, root-mean-square force-fluctuation data, and schlieren motion pictures were obtained at angles of attack from 0° to 12° . The Mach number ranged from 0.5 to 1.0 and the corresponding Reynolds numbers were approximately 1.5×10^6 to 2.1×10^6 .

RESULTS AND DISCUSSION

Pressure Fluctuations

Pressure-pulsation records, as shown in figure 2, were used to obtain typical or predominant values of the double-amplitude pulsating pressures expressed as $\Delta p/q$. The chordwise variation of pressure pulsations on the 9-percent-thick airfoils at several constant normal-force coefficients is presented in figure 3 to show the effect of maximum-thickness location and Mach number on the pressure pulsations. At low normal-force coefficients of 0.2 and 0.4, the maximum pressure pulsations are less than 10 percent of the dynamic pressure and the effect of the location of maximum thickness on pressure pulsations is negligible. At normal-force coefficients of 0.6 and 0.7 the maximum pressure pulsations become significant, reaching values of approximately 30 percent of the stream dynamic pressure. While the NACA 63A009 airfoil has the lowest values of $\Delta p/q$ at a Mach number of 0.5, it shows progressively higher values as the Mach number is increased and has the highest level of pressure pulsations at Mach numbers of 0.9 and 1.0. The NACA 64A009 airfoil has moderately high levels of

$\Delta p/q$ at all Mach numbers, without ever having the lowest values. The NACA 65A009 airfoil, while having high pulsation levels at a Mach number of 0.5, shows the lowest level at Mach numbers from 0.6 to 0.8 and has next to the lowest levels above a Mach number of 0.8. The NACA 16-009 airfoil exhibits high-level pulsations at Mach numbers from 0.5 to 0.8, but has the lowest level at 0.9 and 1.0. Although none of the airfoils investigated had consistently lower pressure-pulsation levels at all Mach numbers, it appears that the NACA 65A009 airfoil would probably offer the best compromise.

Normal-Force-Coefficient Fluctuations

Figure 2 shows a sample record of the pressure pulsations on an NACA 64A009 airfoil at 10° angle of attack and a Mach number of 0.77 and illustrates the phase differences that can occur. Phase differences of as much as 180° between the forward gage and the rear gage are apparent in figure 2, and these large phase differences are responsible for the fact that the root-mean-square fluctuating normal-force coefficient $\overline{\Delta c_n}$ is of smaller magnitude than estimates of this coefficient made from the pressure data without regard for phase relations. Further, these phase differences may produce fluctuations in pitching-moment coefficient.

Before examining the data for normal-force fluctuations in more detail, it is of interest to compare the general level of the force fluctuations with the level of the predominant pressure fluctuations. In order to make such a comparison the $\Delta p/q$ diagrams of figure 3 were integrated to obtain an average value $\overline{\Delta p/q}$ along the chord. This chordwise average value, of course, is arrived at without consideration of phase relations or wave form. Furthermore it is a double-amplitude value by definition. These factors all tend to make $\overline{\Delta p/q}$ several times larger than the measured root-mean-square normal-force-coefficient fluctuation $\overline{\Delta c_n}$.

Figure 4 shows a comparison of $\overline{\Delta p/q}$ with the root-mean-square fluctuating normal-force coefficient $\overline{\Delta c_n}$ for the NACA 64A009 airfoil at several angles of attack over a range of Mach numbers. The curves for $\overline{\Delta p/q}$ have values approximately 5 times those of the curves for $\overline{\Delta c_n}$ for angles of attack up to 6° over most of the Mach number range. At 8° and 10° , the values of the $\overline{\Delta p/q}$ curves increase to 7 times those for the $\overline{\Delta c_n}$ curves. The increase in this ratio from 5 to 7 when going from low to high angle-of-attack ranges is primarily attributed to an increase in the phase difference of the pressures along the chord, since, at the low angles of attack (up to 6°), the pressures have been observed to be more closely in phase (ref. 2) than at angles above 6° , where phase

differences of as much as 180° have frequently been observed (for example, fig. 2).

As previously explained, the $\overline{\Delta p/q}$ curves in figure 4 show double-amplitude values and thus these data should be reduced by a factor of 2 for direct comparison with the curves for the root-mean-square fluctuating normal-force coefficient. When this is done, the $\overline{\Delta p/q}$ data are still approximately 3 times the magnitude of the $\overline{\Delta c_n}$ data. This residual factor includes effects of phase differences, wave form, and also an unknown factor dependent upon the arbitrary method used to select the predominant $\Delta p/q$ values. It is notable that the general level of the normal-force-coefficient fluctuations is low — even at high angles of attack and at Mach numbers between 0.7 and 0.9 the normal-force fluctuations seldom exceed 5 percent of the mean normal force.

The variation of the root-mean-square fluctuating normal-force coefficient $\overline{\Delta c_n}$ with Mach number is presented in figure 5. The general trends of $\overline{\Delta c_n}$ for the airfoils are in agreement with the $\Delta p/q$ data shown in figure 3. For angles of attack up to 6° and for all Mach numbers, the variations of $\overline{\Delta c_n}$ with Mach number are approximately equal for all the airfoils, with the NACA 63A009 and 65A009 airfoils generally having slightly lower values than the other two airfoils. Increasing the angle of attack to 8° produces only a negligible change in the $\overline{\Delta c_n}$ levels for Mach numbers up to 0.725 and this is attributed to the steady nature of the separated flow observed on all the airfoils (fig. 6(a)). Above a Mach number of 0.725, with the flow attempting to attach at the nose, the 6-series airfoils show rapid rises in the normal-force-coefficient fluctuations. The flow attachment occurs on the NACA 16-series airfoil without much unsteadiness and a relatively steady normal-shock formation is obtained, with a steady separated flow aft of the shock, resulting in the generally low root-mean-square normal-force-coefficient fluctuations shown for the NACA 16-series airfoil. At angles of attack above 8° , the behavior of the curves for all the airfoils is similar to that at 6° , except that the levels of $\overline{\Delta c_n}$ are much higher than at lower angles of attack for all Mach numbers, and the $\overline{\Delta c_n}$ rise is more abrupt. The $\overline{\Delta c_n}$ levels do not consistently rise or fall with a systematic variation of the position of maximum thickness, the NACA 64A009 airfoil generally having the highest value of $\overline{\Delta c_n}$ over the Mach number range. A large rise in $\overline{\Delta c_n}$ occurs at angles of attack of 10° and 12° at Mach numbers around 0.7 and is produced by the oscillations of shock and separation point on the airfoils accompanying the unsteady-flow attachment (fig. 6(b)). Lower root-mean-square normal-force-coefficient fluctuations are shown for the NACA 65A009 and 16-009 airfoils because of milder shock and separation-point oscillations and less violent flow movement than for the other airfoils at 10° angle of attack.

Figure 7 shows the variation of the Mach number for the $\overline{\Delta c_n}$ rise with angle of attack and the Mach number for the normal-force break and drag rise. There is no absolute correlation between these three parameters because of the erratic variation of the Mach number for the $\overline{\Delta c_n}$ rise with regard to the other parameters. The $\overline{\Delta c_n}$ rise, however, generally occurs at higher Mach numbers than those for the drag rise but at a Mach number close to that for the lift break.

The variations in $\overline{\Delta c_n}$ with c_n for the four airfoils at various Mach numbers are shown in figure 8. At Mach numbers of 0.5 to 0.85, $\overline{\Delta c_n}$ is not greatly affected by changes in normal-force coefficient up to $c_n = 0.6$, but above $c_n = 0.6$, at values approaching the maximum lift coefficient for the sections, there is a rapid rise in $\overline{\Delta c_n}$. Similar effects were noted in the variation of $\Delta p/q$ with Mach number and normal-force coefficient (fig. 3). When the Mach number is increased above 0.85, the rapid rise in $\overline{\Delta c_n}$ at the higher lift coefficients gradually diminishes and at Mach numbers of the order of 0.98 there is little change in $\overline{\Delta c_n}$ with increasing normal-force coefficient throughout the range. These results indicate that in the region of small changes in $\overline{\Delta c_n}$, which corresponds generally to normal-force coefficients below 0.6, there is little effect of section on the level of force pulsation except at a Mach number 0.5, where the NACA 63A009 and 65A009 airfoils have lower levels. In this region of normal-force coefficients approaching maximum lift, where the fluctuating load is increasing rapidly, the values of $\overline{\Delta c_n}$ measured on the NACA 65A009 airfoil were smaller than those measured on the other airfoils. Similar effects are noted in figure 9, where the normal-force coefficient and Mach number at which the pulsating normal force exceeds the specific values of 0.012, 0.014, and 0.016 are shown for the various sections. These results also show no consistent effect of changes in maximum-thickness location; however, at high Mach numbers the NACA 65A009 airfoil, in general, showed high c_n levels for specific values of $\overline{\Delta c_n}$ throughout the Mach number range.

Figure 10 is a summary plot presenting the effects of maximum-thickness location for three 6-series airfoils and one unrelated 16-series airfoil on $\overline{\Delta c_n}$ for several constant normal-force coefficients. The variation of $\overline{\Delta c_n}$ with maximum-thickness location is characterized by peak values of $\overline{\Delta c_n}$ occurring around the 39-percent-chord maximum-thickness location (NACA 64A009 airfoil), while the airfoils using a forward or a more rearward maximum-thickness location generally show lower values of $\overline{\Delta c_n}$. The airfoils having a maximum-thickness location at or behind the 42.5-percent-chord station (NACA 65A009 and 16-009) generally had the lowest levels of $\overline{\Delta c_n}$, except at $c_n = 0.2$, where the levels of $\overline{\Delta c_n}$ are of limited significance.

CONCLUDING REMARKS

A two-dimensional wind-tunnel investigation of the effects of the location of maximum thickness on pressure pulsations and root-mean-square force fluctuations on three 6-series airfoils and one 16-series airfoil of 9-percent thickness indicated that:

1. Marked variations were found in the phase relationships of the pressures at the various chordwise stations. Thus, the average pulsating pressure along the chord cannot be used as an average value of the fluctuating normal force. From the present results it appears that the correct root-mean-square value of the normal-force-coefficient fluctuations is of the order of one-third of the value estimated from a chordwise average of the predominant pressure fluctuations by assuming all of the pressure fluctuations to be in phase. The results also indicated that phase differences tend to become more pronounced at the higher angles of attack.

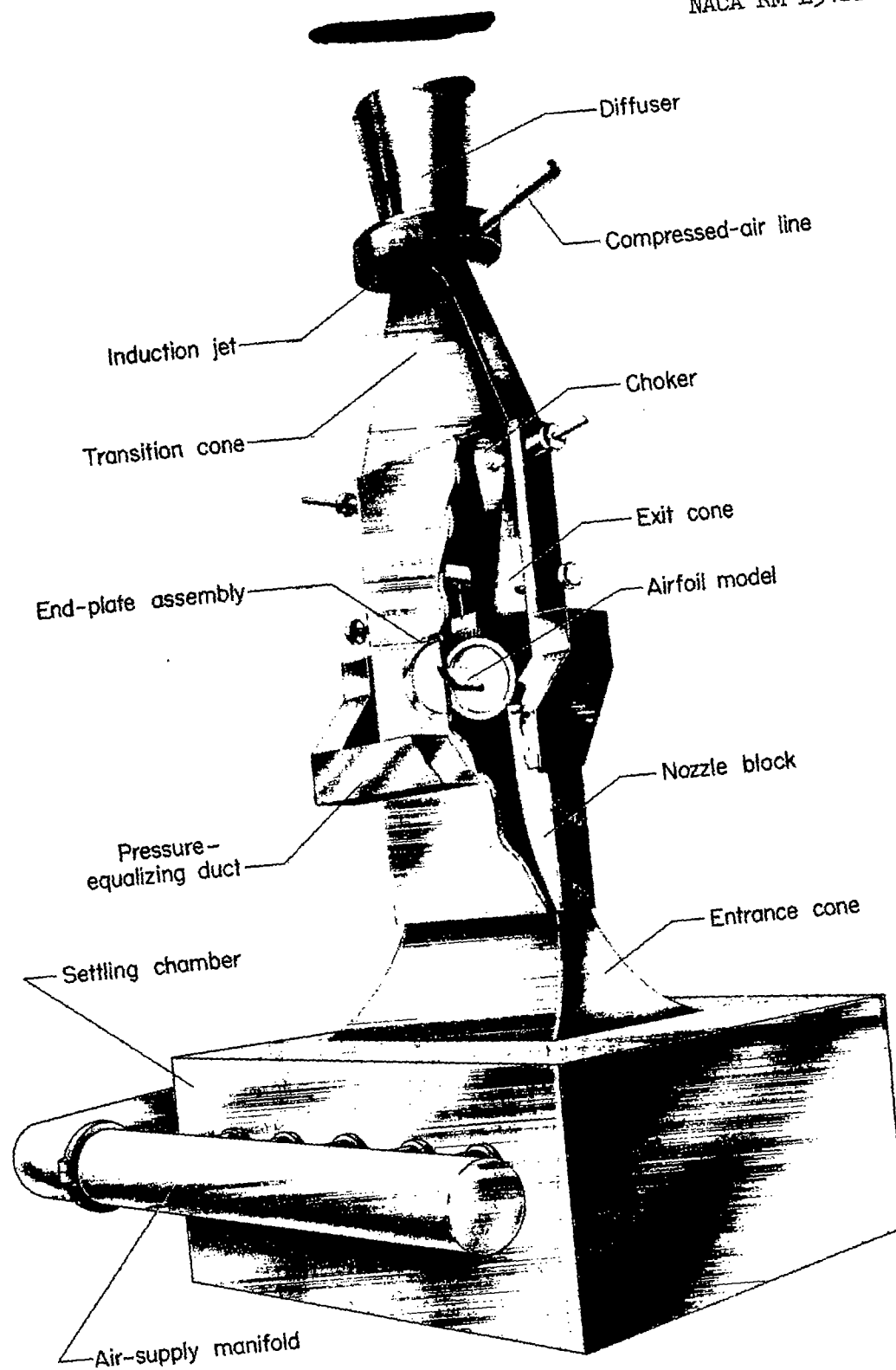
2. The largest normal-force fluctuations, which occurred in the Mach number range from 0.7 to 0.9 at the highest test angles of attack, seldom exceeded about 5 percent of the mean normal force. A comparison of the root-mean-square force-fluctuation levels for four 9-percent-thick airfoils (NACA 63A009, 64A009, 65A009, and 16-009) revealed no marked differences at normal-force coefficients up to about 0.6. At higher values of normal-force coefficient, however, the NACA 65A009 and NACA 16-009 airfoils, which had more rearward maximum-thickness positions than the other two sections, had lower levels of fluctuating normal force.

3. From the standpoint of local panel loads, none of the airfoils had consistently lower loads throughout the speed and normal-force-coefficient ranges. It appeared, however, that the NACA 65A009 airfoil would probably be the best choice of the sections tested for operation throughout the high subsonic Mach number range.

Langley Aeronautical Laboratory,
National Advisory Committee for Aeronautics,
Langley Field, Va., February 10, 1954.

REFERENCES

1. Humphreys, Milton D., and Kent, John D.: The Effects of Camber and Leading-Edge-Flap Deflection on the Pressure Pulsations on Thin Rigid Airfoils at Transonic Speeds. NACA RM L52G22, 1952.
2. Humphreys, Milton D.: Pressure Pulsations on Rigid Airfoils at Transonic Speeds. NACA RM L51I12, 1951.
3. Coe, Charles F., and Mellenthin, Jack A.: Buffeting Forces on Two-Dimensional Airfoils As Affected by Thickness and Thickness Distribution. NACA RM A53K24, 1954.
4. Daley, Bernard N., and Dick, Richard S.: Effect of Thickness, Camber, and Thickness Distribution on Airfoil Characteristics at Mach Numbers Up to 1.0. NACA RM L52G31a, 1952.
5. Katzoff, S., Gardner, Clifford S., Diesendruck, Leo, and Eisenstadt, Bertram J.: Linear Theory of Boundary Effects in Open Wind Tunnels With Finite Jet Lengths. NACA Rep. 976, 1950. (Supersedes NACA TN 1826.)
6. Helfer, Arleigh P.: Electrical Pressure Integrator. NACA TN 2607, 1952.



L-83293

Figure 1.- Langley 4- by 19-inch semiopen tunnel.

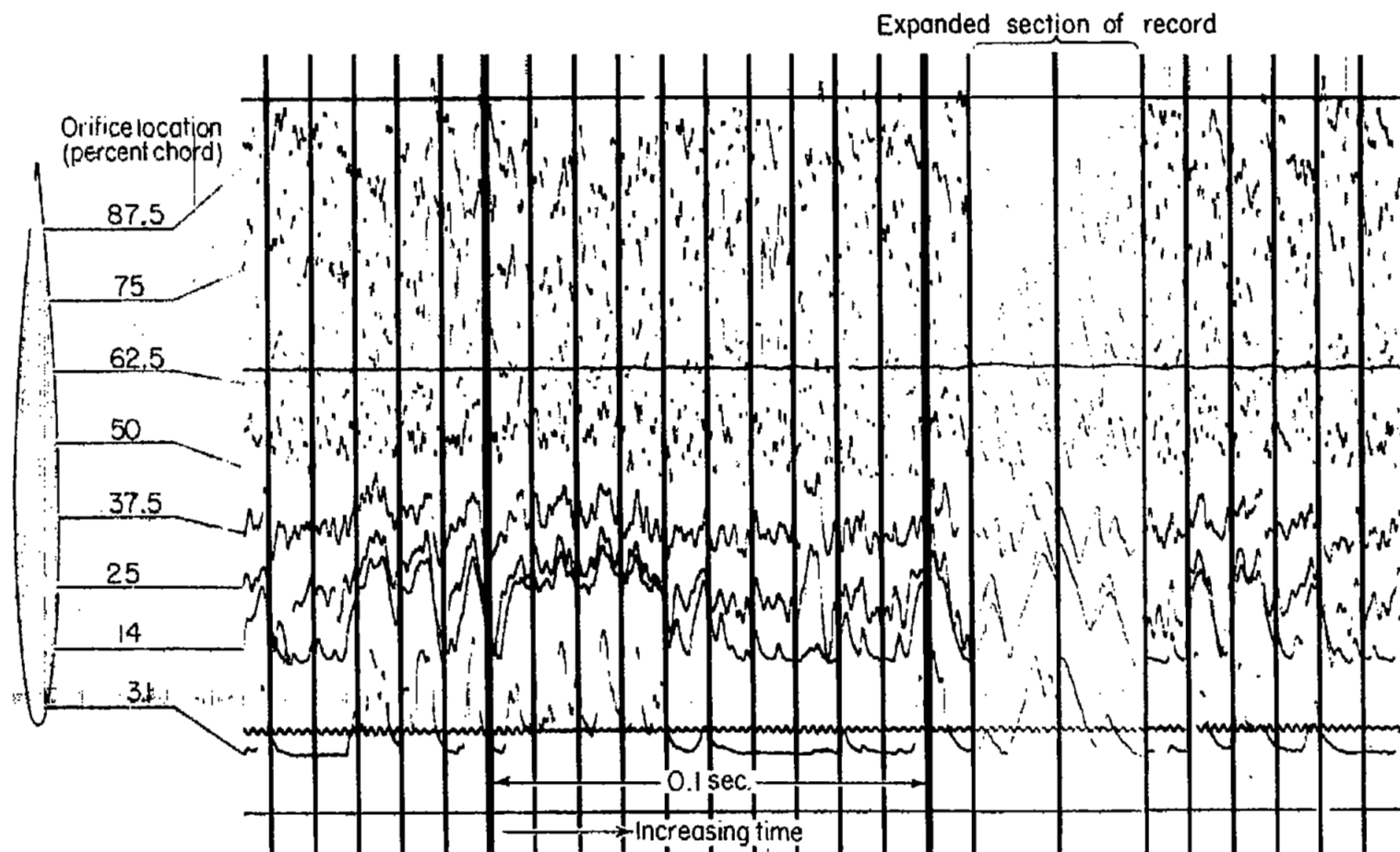


Figure 2.- Typical pressure pulsations on an NACA 64A009 airfoil, illustrating phase differences that occur. $\alpha = 10^\circ$; $M = 0.77$.

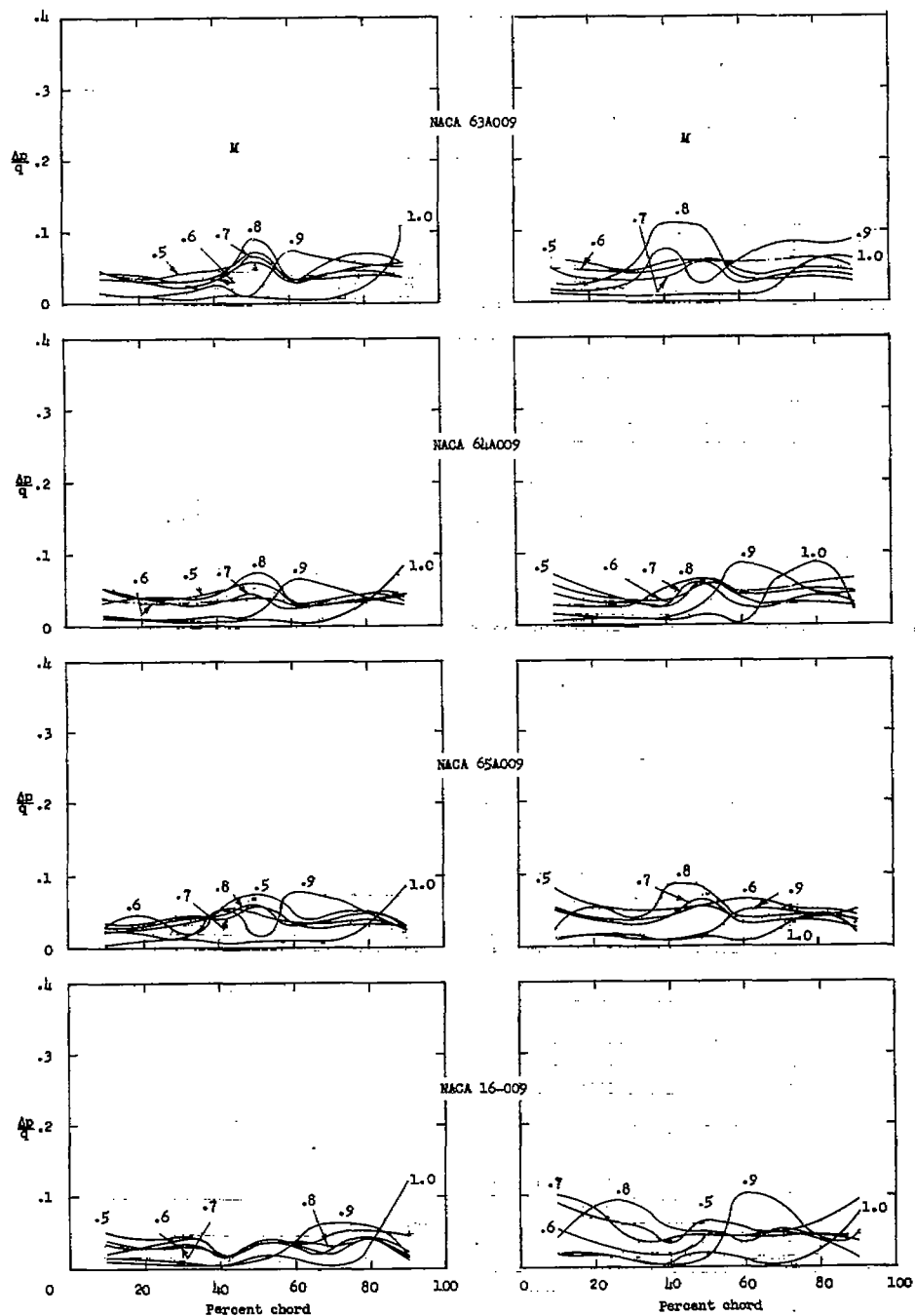
(a) $c_n = 0.2$.(b) $c_n = 0.4$.

Figure 3.- The effect of maximum-thickness location and Mach number on the chordwise pressure pulsations on 9-percent-thick NACA airfoils at several constant normal-force coefficients.

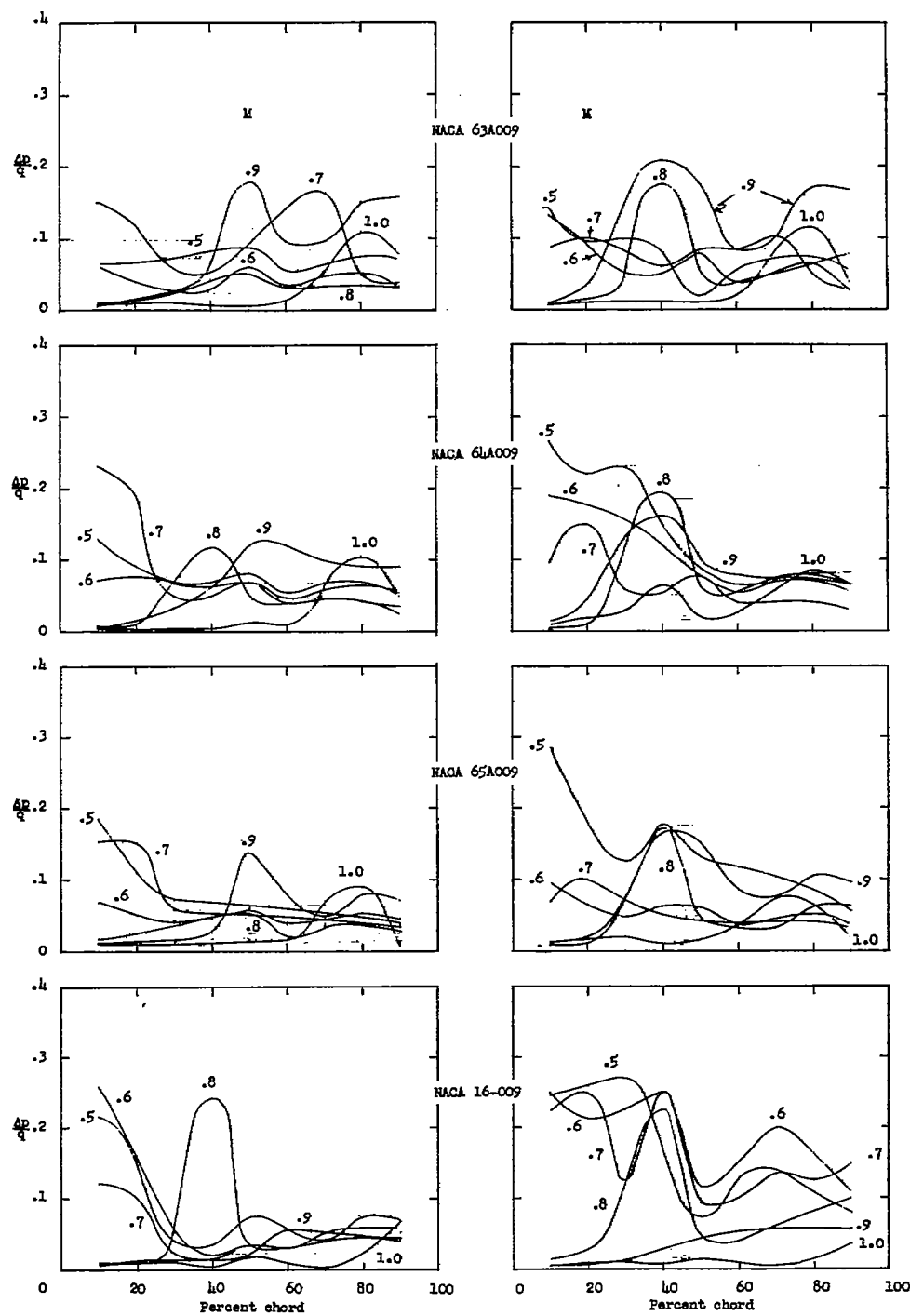
(c) $c_n = 0.6$.(d) $c_n = 0.7$.

Figure 3.- Concluded.

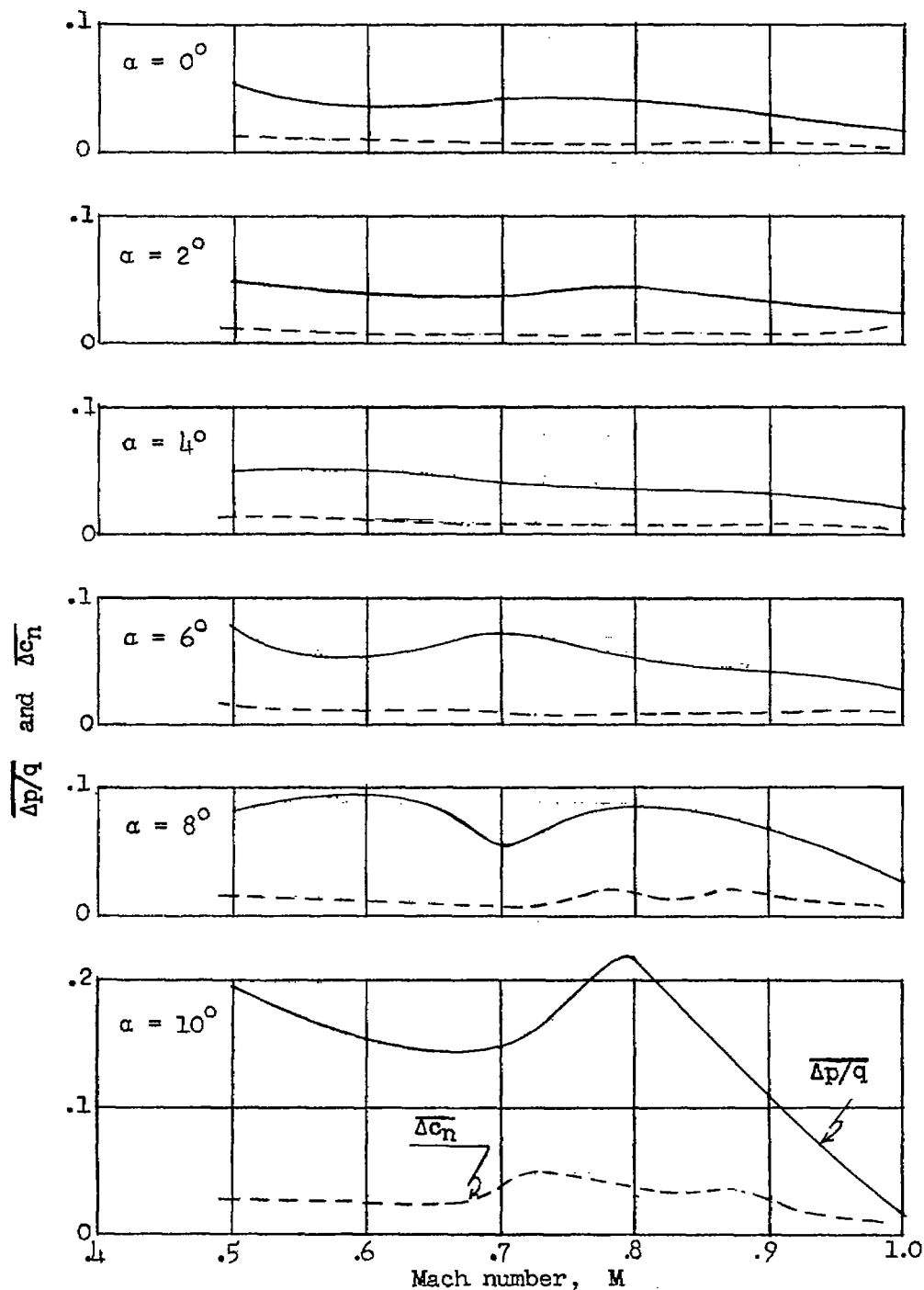


Figure 4.- Comparison of $\overline{\Delta p/q}$ with root-mean-square fluctuating normal-force coefficient for the NACA 64A009 airfoil at several angles of attack over a range of Mach numbers.

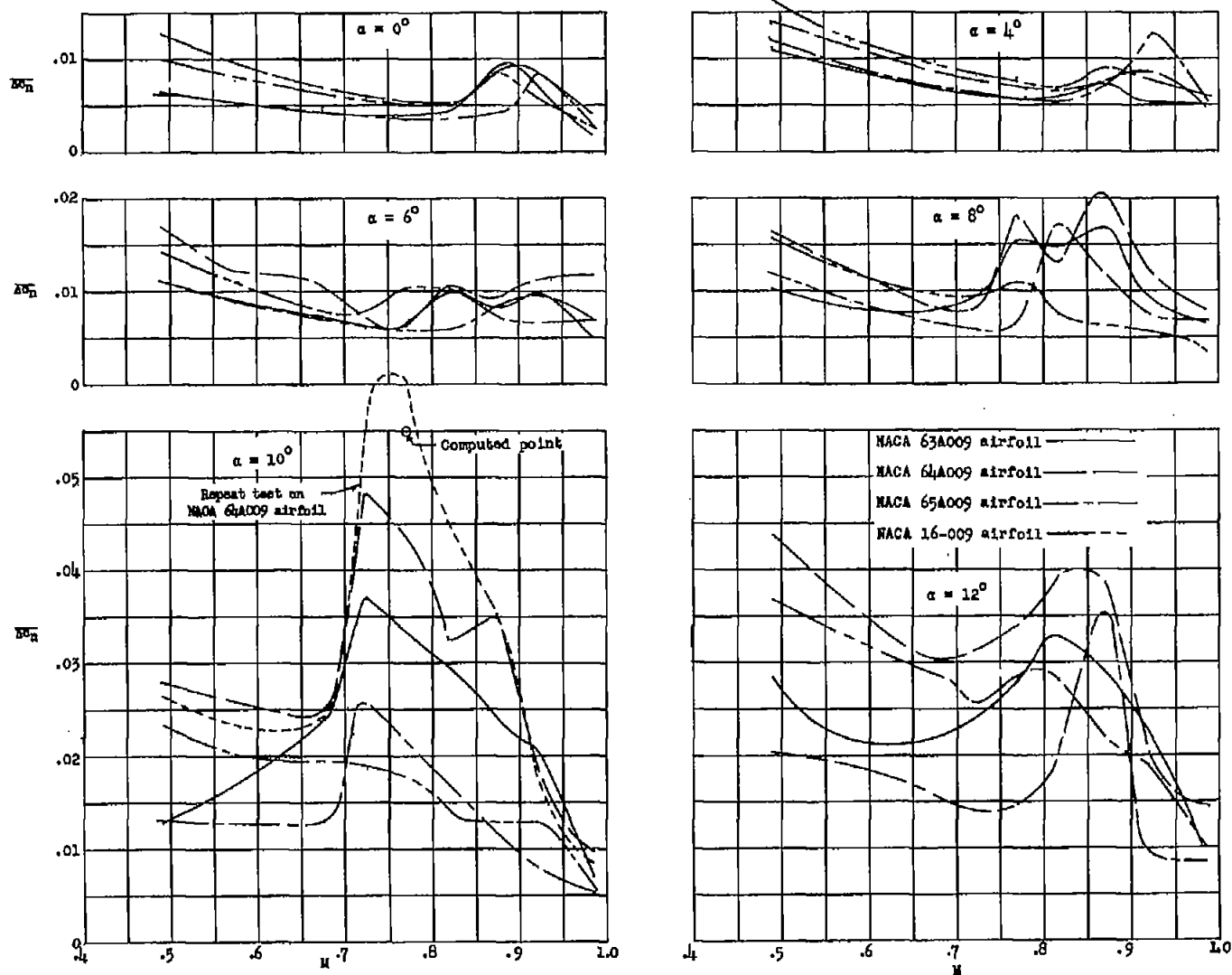


Figure 5.- The variation of root-mean-square fluctuating normal-force coefficient with Mach number.



L-83291.1

NACA 64A009

NACA 65A009

(a) $\alpha = 10^\circ$; $M = 0.65$.

Figure 6.- Schlieren motion-picture photographs; 250 frames per second.



NACA 64A009

NACA 65A009

L-83292.1

(b) $\alpha = 10^\circ$; $M = 0.77$.

Figure 6.- Concluded.

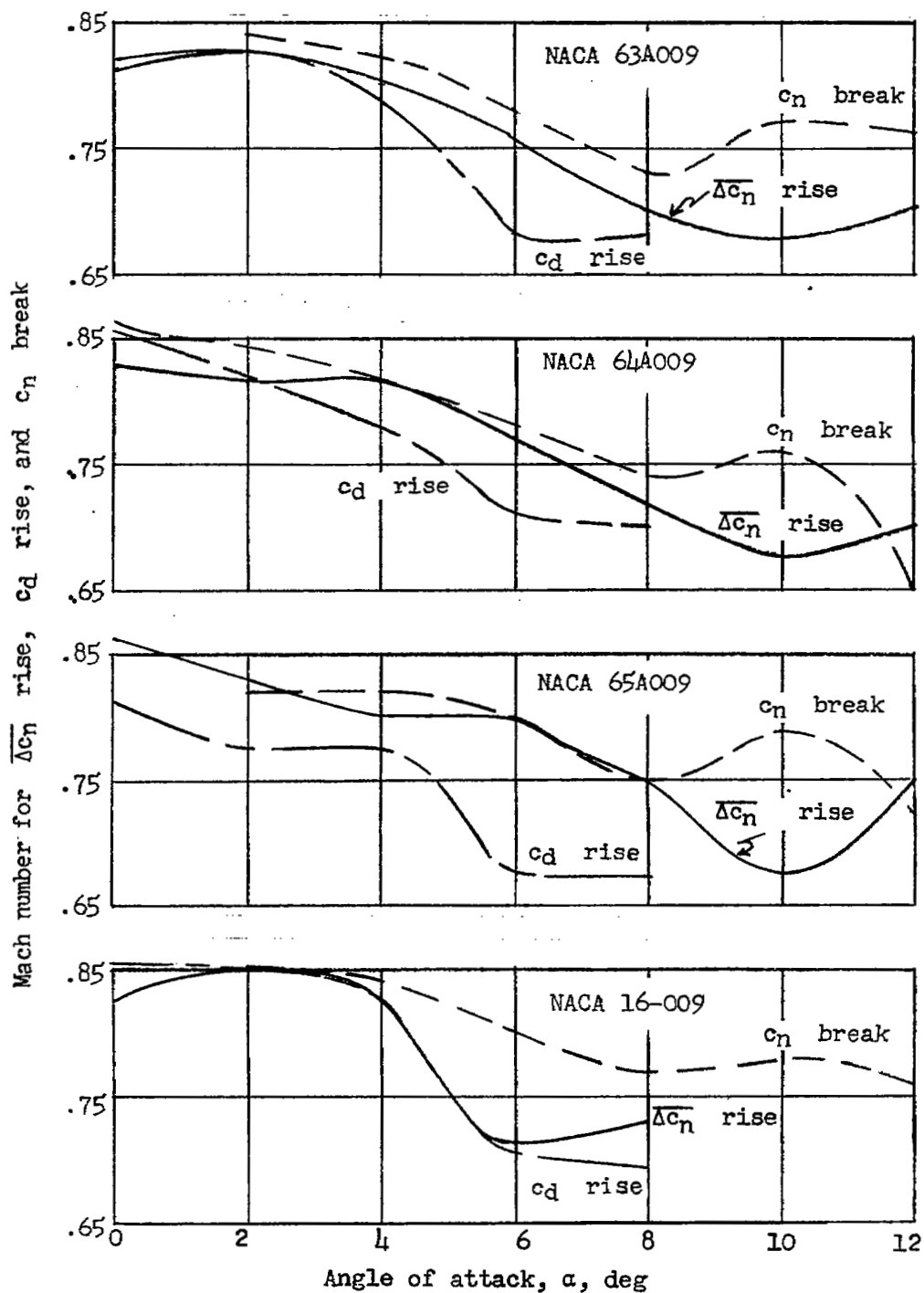
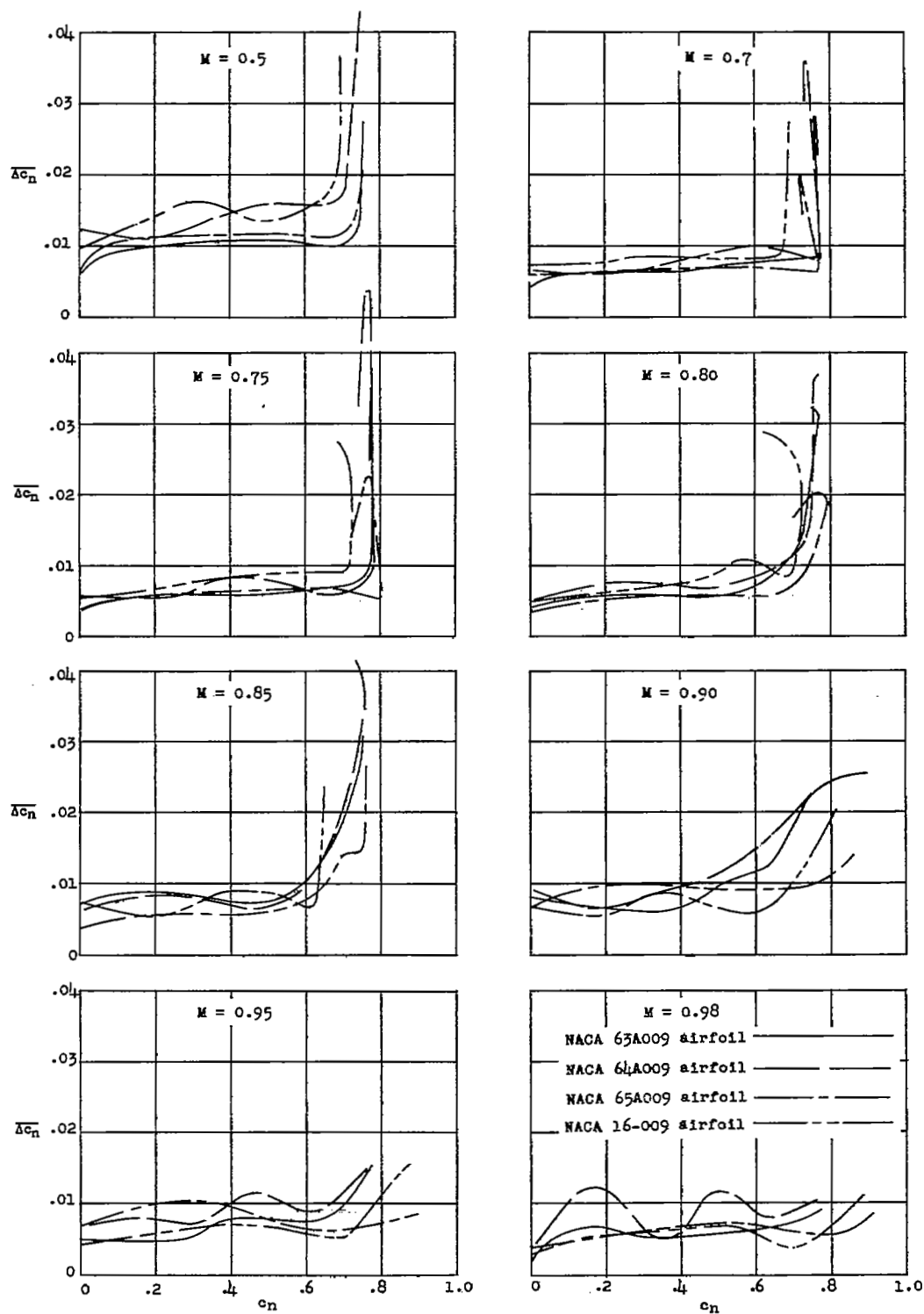


Figure 7.- Comparison of Mach number for occurrence of Δc_n rise with Mach number for drag rise and normal-force break.



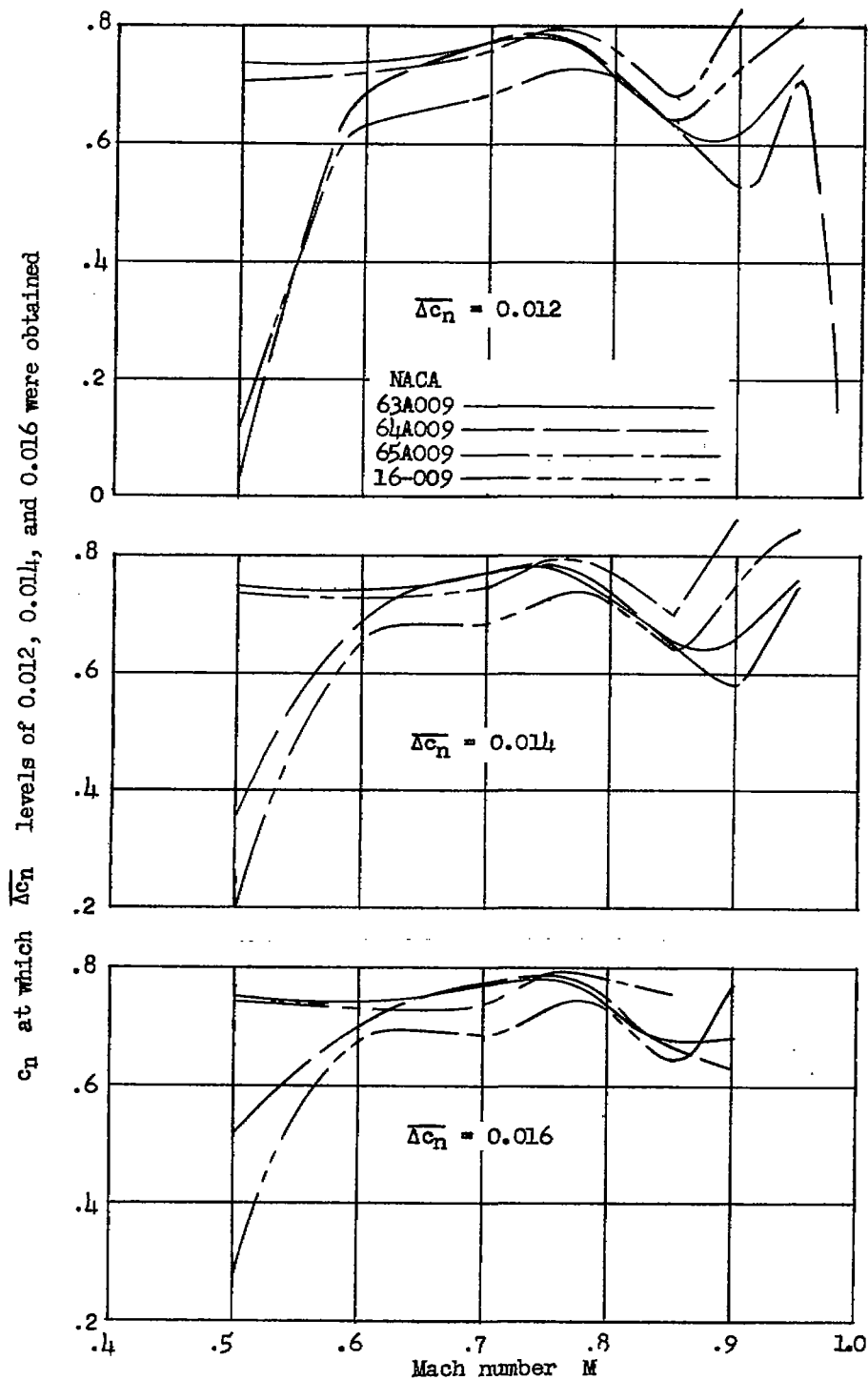


Figure 9.-- Normal-force coefficient at which $\overline{\Delta c_n}$ values of 0.012, 0.014, and 0.016 are first obtained.

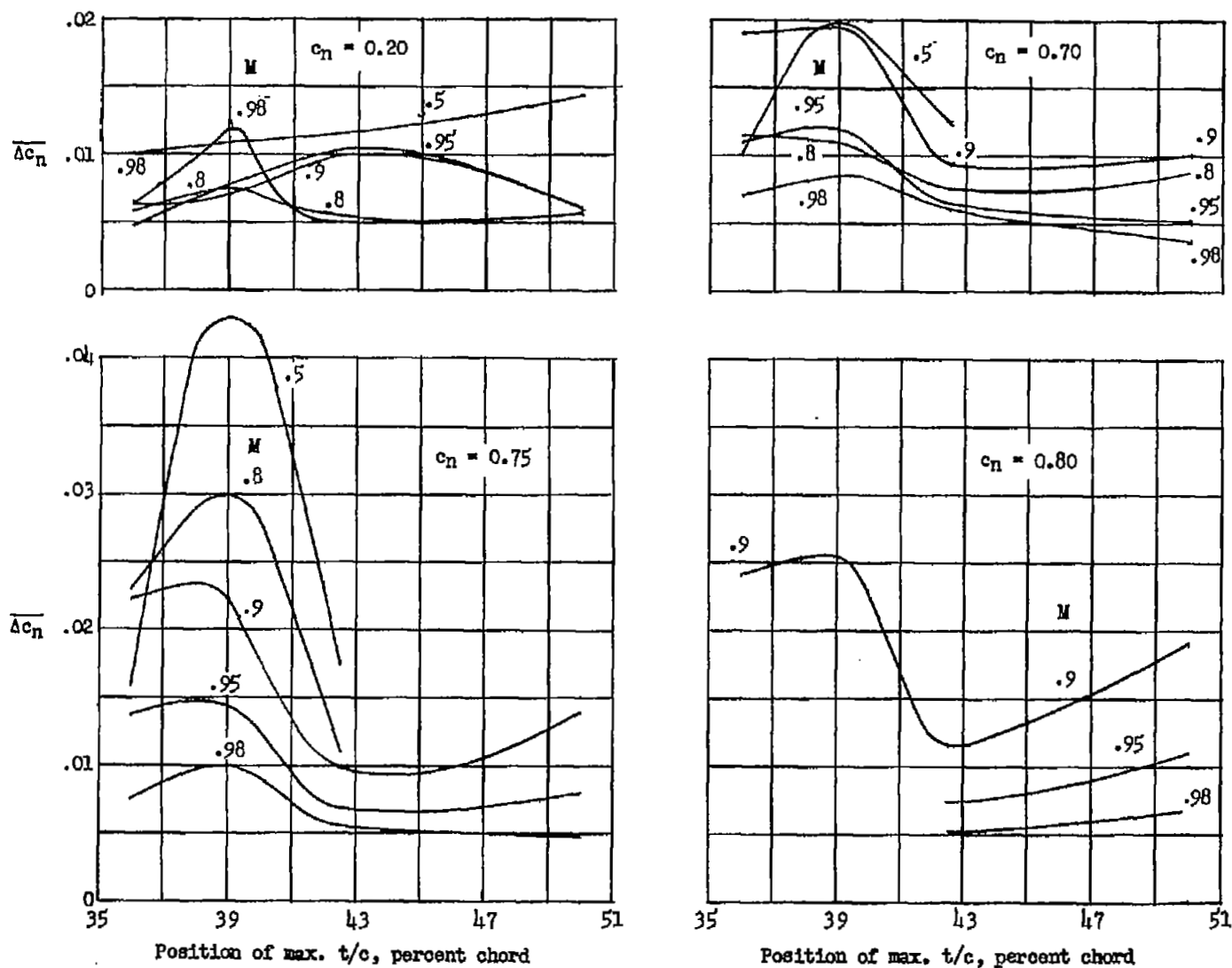


Figure 10.- Effect of maximum-thickness location on Δc_n .

[REDACTED]

NASA Technical Library

3 1176 01437 1364

[REDACTED]

[REDACTED]

[REDACTED]